J|A|C|S
ARTICLES
Published on Web 03/14/2002

Chemical Control of Phase Transformation Kinetics in Periodic Silica/Surfactant Composites

Adam F. Gross, Van H. Le, Bradley L. Kirsch, and Sarah H. Tolbert*

Contribution from the Department of Chemistry and Biochemistry, University of California, Los Angeles, Los Angeles, California 90095-1569

Received August 29, 2001

Abstract: Control of phase stability is investigated through control of silica chemistry in ordered silica/surfactant composites under hydrothermal conditions. The composites were hydrothermally treated in pH 9 through pH 11 buffers while using in situ real time X-ray diffraction to follow a *p*6*mm* hexagonal-to-lamellar structural transition. The data were analyzed using both isothermal and nonisothermal (temperature-ramped) kinetics to determine activation energies. It was found that the most mildly basic conditions utilized (pH 9), which favor silica condensation, best inhibit the phase transition and thus produce the most kinetically stable composites. High-pH treatment, conversely, allows for the most facile rearrangements. Condensation occurring during composite synthesis rather than during hydrothermal treatment has a much smaller effect on phase stability, probably because much of the condensation that occurs during synthesis is random and not optimally coupled to the nanoscale architecture. Materials that start out poorly condensed, by contrast, can be extensively hydrothermally modified so that the final material has an inorganic framework with a highly uniform silica density; this provides the maximum resistance to transformation and the highest kinetic stability. In all cases, very good agreement is found between the results of isothermal and nonisothermal kinetic methods. The trends across pHs indicate that both isothermal and nonisothermal measurements are accurate and that differences between them are meaningful and represent physical differences in the transforming materials resulting from the different heating processes.

Introduction

Activation energies represent the quantity of energy necessary to overcome a barrier to reach a new chemical or physical state. Usually, solution-phase chemistry cannot be utilized to modify activation energies for crystalline solids because chemically altering the sample also changes the crystal phase of the material. However, in materials such as silica/surfactant composites (MCM-41-type materials), it is possible to hydrothermally modify the atomic scale amorphous silica framework without changing the nanoscale periodicity of the composite.[1−12] Careful examination of the nanometer scale architecture, however, shows that these atomic scale changes do influence the nanoscale structure in subtle ways.[3,4,13,14] If these inorganic/organic composite materials undergo a rearrangement of the nanometer scale periodicity after chemical framework alteration, they can show markedly different transformation kinetics.[3,15−17] By controlling the possible chemical reactions in the transforming material and observing the effect on activation energies, we are thus able to identify the experimental variables that control metastability.

Once it is understood which chemical parameters most heavily influence phase stability, it becomes possible to identify the physical changes that result in the altered kinetics. By identifying changes that inhibit or accelerate rearrangements, we can gain a better understanding of the actual molecular and atomic motions that occur during a rearrangement. This both increases fundamental understanding about transformation mechanisms in inorganic/organic composite materials and provides insight into the design of synthetic pathways that utilize structural rearrangements to create new materials.[17−20]

* To whom correspondence should be addressed. E-mail: tolbert@chem.ucla.edu.

(1) Kresge, C. T.; Leonowitz, M. E.; Roth, W. J.; Vartuli, J. C.; Beck, J. S. *Nature* **1992**, *359*, 710. Beck, J. S.; Vartuli, J. C.; Roth, W. J.; Leonowicz, M. E.; Kresge, C. T.; Schmitt, K. T.; Chu, C. T.-W.; Olson, D. H.; Sheppard, E. W.; McCullen, S. B.; Higgins, J. B.; Schlenker, J. L. *J. Am. Chem. Soc.* **1992**, *114*, 10834.
(2) Huo, Q.; Margolese, D. I.; Stucky, G. D. *Chem. Mater.* **1996**, *8*, 1147.
(3) Gross, A. F.; Ruiz, E. J.; Tolbert, S. H. *J. Phys. Chem. B* **2000**, *104*, 5448.
(4) Gross, A. F.; Le, V. H.; Kirsch, B. L.; Riley, A. E.; Tolbert, S. H. *Chem. Mater.* **2001**, *13*, 3571.
(5) Ryoo, R.; Jun, S. *J. Phys. Chem. B* **1997**, *101*, 317.
(6) Kim, J. M.; Jun, S.; Ryoo, R. *J. Phys. Chem. B* **1999**, *103*, 6200.
(7) Elder, K. J.; White, J. W. *Chem. Mater.* **1997**, *9*, 1226.
(8) Kruk, M.; Jaroniec, M.; Sayari, A. *Microporous Mesoporous Mater.* **1999**, *27*, 217.
(9) Kruk, M.; Jaroniec, M.; Sayari, A. *J. Phys. Chem. B* **1999**, *103*, 4590.
(10) Wu, J.; Liu, X.; Tolbert, S. H. *J. Phys. Chem. B* **2000**, *104*, 11837.
(11) Lin, H.-P.; Mou, C.-UJ.; Liu, S.-B.; Tang, C.-Y.; Lin, C.-Y. *Microporous Mesoporous Mater.* **2001**, *44*−*45*, 129.
(12) Feng, P.; Bu, X.; Pine, D. J. *Langmuir* **2000**, *16*, 5304.
(13) Impéror-Clerc, M.; Davidson, P.; Davidson, A. *J. Am. Chem. Soc.* **2000**, *122*, 11925.
(14) Elder, K. J.; Reynolds, P. A.; White, J. W.; Cookson, D. *J. Chem. Soc., Faraday Trans.* **1997**, *93*, 199.
(15) Gross, A. F.; Le, V. H.; Kirsch, B. L.; Tolbert, S. H. *Langmuir*, **2001**, *17*, 3496.
(16) Tolbert, S. H.; Landry, C. C.; Stucky, G. D.; Chmelka, B. F.; Norby, P.; Hanson, J. C.; Monnier, A. *Chem. Mater.* **2001**, *13*, 2247.
(17) Landry, C. C.; Tolbert, S. H.; Gallis, K. W.; Monnier, A.; Stucky, G. D.; Norby, P.; Hanson, J. C. *Chem. Mater.* **2001**, *13*, 1600.
(18) Gallis, K. W.; Landry, C. C. *Chem. Mater.* **1997**, *9*, 2035.
(19) Pevzner, S.; Regev, O. *Microporous Mesoporous Mater.* **2000**, *38*, 413.

The material used in the work is a silica/surfactant composite synthesized with a 20-carbon-alkane-tailed trimethylammonium surfactant, which undergoes a *p*6*mm* hexagonal-to-lamellar phase transition. The rearrangement appears to be driven by changes in surfactant curvature.[15,21] When the surfactant is heated, the alkane tail becomes thermally excited and takes up more volume.[22] The result of this tail disorder is to lower the surfactant curvature, which then drives the composite toward a structure with lower curvature organic domains such as a lamellar structure. The rigid silica framework opposes the surfactant shape change and favors the starting hexagonal configuration of the material. A material with increased initial polymerization resists a phase transition,[3] but the results presented herein show that a composite material that undergoes significant framework condensation during heating prior to the phase change shows even better resistance to change.

On the basis of our prior work, we believe that condensation of silica bonds during hydrothermal treatment should have a major effect on phase stability in hexagonal silica/surfactant composites.[3,4,15] We test this hypothesis by controlling the silica chemistry occurring during the hydrothermal treatment and analyzing the kinetics of transformation. Silica chemistry has a strong dependence on pH. At neutral pHs, condensation is fast, while hydrolysis is very slow;[23] the opposite trend is seen at high pH. In our experiment, the hydrothermal solution is buffered to control silica chemistry at all times. This is advantageous because hydroxide released or utilized during hydrothermal treatment can dramatically alter the solution pH.

Varying pH has been shown in previous work on silica/surfactant mesophases to alter phase stability and framework flexibility. For example, synthesis pH has been used to control the final product of composite syntheses under basic conditions.[20] Low base concentrations resulted in hexagonal structures, medium and very high base concentrations produced lamellar composites, and moderately high base concentrations were utilized to form cubic materials. Another example of pH altering phase stability is experiments where acidic preparation silica/surfactant thin films were made with an internal photoacid generator. Irradiation of the films during drying caused a decrease in pH that drove a hexagonal-to-tetragonal phase change.[24] Both of these experiments emphasize how silica charge, which is controlled by solution pH, may be used to alter the final order in the material. In addition, silica polymerization, which affects the ease of rearrangement, is affected by pH.[4,15] For example, 150 °C high-pH hydrothermal treatment allows pore expansion and maintains periodic order in a hexagonal composite material, while treatment at neutral pH under the same conditions results in less pore expansion and a badly ordered final product.[8,9,25−29] Other work has shown that hydrothermal treatment at various basic pHs controls the intensity of the Bragg scattering from the nanometer-scale structure.[7] Particularly in the synthesis of *Ia*3*d* cubic composites, which are frequently formed through a hydrothermal phase transformation process, solution pH has been shown to have a dramatic affect on the time and temperature needed to form this structure.[16,17,19,20] All of these results show that pH is an important factor in determining composite structural malleability; however, few systematic studies of the effect of pH on phase stability or transformation kinetics during hydrothermal restructuring have been performed.

In this work, we use both in situ and ex situ techniques to understand the physical changes occurring in composites during a hexagonal-to-lamellar phase transformation. To understand how local bonding changes upon hydrothermal treatment, ex-situ ^{29}Si MAS NMR was utilized. These experiments allow us to correlate kinetic changes with altered bonding in our materials. In situ low-angle X-ray diffraction (XRD) was used to follow structural changes on the nanometer length scale in the material. This technique has successfully been used before to quantify structural changes in silica/surfactant composite materials.[3,4,15,30−32] In our work, the XRD data are fit to multiple kinetic models to try to understand how to best analyze a complex system such as this. In these experiments, we heat the hydrothermal composite mixture both isothermally (rapid temperature jump to a set point followed by a hold) and on a linear temperature ramp (nonisothermally) and compare the results. The goal is both to learn about the chemical and physical changes that occur during each thermal history and to assess the applicability of each method to the study of complex nanostructured materials.

The heating profile of a material prior to transformation is important in determining what type of chemistry can occur.[15] Nonisothermal heating employs relatively slow ramps and takes data during the temperature rise. There is significant time for the framework to react with the hydrothermal solution at low temperatures during heating. By contrast, during isothermal heating, the temperature quickly jumps to a set value and is held at that value. As a result, a larger fraction of the silica condensation or hydrolysis occurs at high temperatures. This favors higher activation energy processes relative to more kinetically facile processes. Both heating methods have been used in the literature; however, very few comparisons of isothermal and nonisothermal kinetic analyses exist.[33−35] Because atomic scale chemistry is not tied by symmetry to nanometer scale rearrangements in these materials, differences in silica chemistry caused by different heating profiles have the potential to dramatically alter transition kinetics.

Many early kinetic experiments employed either differential scanning calorimetry (DSC) or differential thermal analysis (DTA), which are indirect measurements of the population of

(20) Xu, J.; Luan, Z.; He, H.; Zhou, W.; Kevan, L. *Chem. Mater.* **1998**, *10*, 3690.
(21) Lapeña, A. M.; Gross, A. F.; Tolbert, S. H., to be submitted for publication.
(22) Israelachvili, J. N. *Intermolecular and Surface Forces*, 2nd ed; Academic Press: London, 1992.
(23) Iler, R. K. *The Chemistry of Silica: Solubility, Polymerization, Colloid and Surface Properties, and Biochemistry*; Wiley: New York, 1979.
(24) Doshi, D. A.; Huesing, N. K.; Lu, M.; Fan, H.; Lu, Y.; Simmons-Potter, K.; Potter, B. G.; Hurd, A. J.; Brinker, C. J. *Science* **2000**, *290*, 107.
(25) Sayari, A.; Liu, P.; Kruk, M.; Jaroniec, M. *Chem. Mater.* **1997**, *9*, 2499.
(26) Sayari, A.; Kruk, M.; Jaroniec, M.; Moudrakovski, I. L. *Adv. Mater.* **1998**, *10*, 1376.
(27) Corma, A.; Kan, Q.; Navarro, M. T.; Perez-Pariente, J.; Rey, F. *Chem. Mater.* **1997**, *9*, 2123.
(28) Kruk, M.; Jaroniec, M.; Sayari, A. *Microporous Mesoporous Mater.* **2000**, *35*−*36*, 545.
(29) Sayari, A. *Angew. Chem., Int. Ed.* **2000**, *39*, 2920.
(30) Lindén, M.; Ågren, P.; Karlsson, S.; Bussian, P.; Amenitsch, H. *Langmuir* **2000**, *16*, 5831.
(31) Ågren, P.; Lindén, M.; Rosenholm, J. B.; Blanchard, J.; Schüth, F.; Amenitsch, H. *Langmuir* **2000**, *16*, 8809.
(32) Ågren, P.; Lindén, M.; Rosenholm, J. B.; Schwarzenbacher, R.; Kriechbaum, M.; Amenitsch, H.; Laggner, P.; Blanchard, J.; Schüth, F *J. Phys. Chem. B* **1999**, *103*, 5943.
(33) Ozawa, T. *Bull. Chem. Soc. Jpn.* **1965**, *38*, 1881.
(34) Donald, I. W. *J. Mater. Sci.* **1995**, *30*, 904.
(35) Abdel-Rahim, M. A.; Ibrahim, M. M.; Dongol, M.; Gaber, A. *J Mater. Sci.* **1992**, *27*, 4685.

each phase. With the advent of modern synchrotron sources, it is now possible to directly determine the population of each phase present in the sample.[3,15−17,36−40] More detail is obtained from XRD and higher accuracy fits to the data are now possible. By comparing our isothermal and nonisothermal data, we hope to discover the advantages and drawbacks of each kinetic method for analyzing complex chemical systems. We note that, while our work is centered on a specific hexagonal-phase silica/surfactant composite, the conclusions regarding hydrothermal silica chemistry should apply to many types of nanostructured silica-based materials. More broadly, a better understanding of chemical control of phase transitions should give insight into understanding phase stability in a wide range of nanoscale composite materials where atomic and nanoscale rearrangements can occur independently.[41] Our conclusions may also make it easier to choose an appropriate kinetic method for analyzing phase transformations observed using in situ X-ray diffraction.

Experimental Section

The synthesis of the silica/surfactant composites used in this work has been described previously.[2,3] Briefly, samples were synthesized using TEOS as a silica source and an eicosyltrimethylammonium bromide surfactant and were made with two concentrations of base; higher synthesis base concentration materials (0.235 M NaOH) have less polymerized frameworks and are referred to as "less initially condensed samples", while lower synthesis base concentration (0.150 M NaOH) materials have more polymerized frameworks and are referred to as "more initially condensed samples".[4,15,42] Control of pH during hydrothermal treatment was achieved using a 0.250 M boric acid/borate buffer. Buffers of pH 9, 10, and 11 were 0.250 M in H_3BO_3 and 0.111, 0.200, and 0.243 M in tetraethylammonium hydroxide, respectively. The electron-deficient nature of the borate anion appeared to minimize undesirable chemistry between the anion and the quaternary ammonium surfactant. Less initially condensed samples treated at a specific pH are called pH *X* samples (where *X* is the treatment pH), while more initially condensed samples treated at a specific pH are called pH *X*c samples (c for condensed). For example, a pH 10-treated composite made with 0.235 M NaOH is called a "pH 10 sample", while a pH 10-treated composite made with 0.150 M NaOH is called a "pH 10c sample".

Structural changes were followed using real time X-ray powder diffraction. Data were collected while heating composites in a buffer slurry under hydrothermal conditions. Either a slow linear temperature ramp or a quick ramp to a holding temperature followed by a temperature hold was employed; quick ramps totaled 2 min in duration. In situ low-angle scattering was collected using 9 keV synchrotron radiation (SSRL) and an X-ray CCD camera to time slice the diffraction during heating. The details of the diffraction and heating setup have been presented elsewhere.[3,15,43] Multiple ramp rates and heating temperatures were used to examine kinetic effects on the phase transition. All diffraction peaks were fit to Voigt functions to find peak areas and positions.

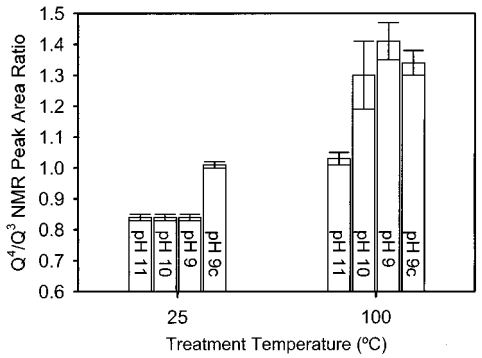

Figure 1. Framework polymerization for composites heated at 4.4 °C/min in buffered aqueous solutions. The treatment pH is indicated on the plot. Less initially condensed samples show increasing condensation with decreasing treatment pH in agreement with established trends in silica chemistry. While the more initially condensed sample (pH 9c) starts more polymerized, it shows less change than the less initially condensed sample heated at the same pH (pH 9) because the more polymerized framework is less flexible and cannot easily reorganize.

Composites were characterized with ^{29}Si MAS NMR using a Bruker Avance 300 spectrometer with a standard one-pulse acquisition and a 240 s recycle delay.[4] Samples used for NMR spectroscopy were used as-synthesized or were hydrothermally heated to 100 °C in sealed ampules in a 1.4 °C/min temperature-ramped oil bath.[4] After heating, samples were rapidly quenched to room temperature and filtered for NMR analysis as dry powders.

Results

Our goal is to better understand how chemical changes that occur during hydrothermal heating affect the ability of silica/surfactant composite materials to rearrange their nanoscale architecture. To achieve this, we will first explore the atomic scale changes that result from heating in different hydrothermal environments and then discuss the effect of this chemistry on the ability of the samples to alter long-range periodicity.

Changes in Atomic Scale Bonding. Silica chemistry varies substantially over the pH range used in this experiment.[23] Condensation is much faster at pH 9 than at pH 11.[23] The hydrolysis of Si−O−Si bonds has an opposite trend, with a minimal hydrolysis rate observed at pH 9. These trends agree with changes in composite framework condensation seen in Figure 1, which shows Q^4/Q^3 peak area ratios from ^{29}Si MAS NMR for samples ramp-heated under different pH conditions at 1.4 °C/min to 100 °C. The Q^4 peak indicates a Si bonded to four other Si atoms through O bridges and is the limit of a fully condensed silica structure. The Q^3 peak indicates three Si−O−Si bonds and one terminal Si−O$^-$ or Si−OH; Q^3 Si represents either a defect or part of the very large interfacial area always present in these composites. A larger Q^4/Q^3 integrated area ratio indicates a more polymerized sample. All samples show a net increase in polymerization on heating from 25 to 100 °C as evidenced by the increase in Q^4/Q^3 ratios. Both the less and more initially condensed samples show pH-dependent changes. In agreement with our chemical intuition, however, the magnitude of the change is greater in less initially condensed samples (Figure 1, pH 9 versus pH 9c samples). While the more initially condensed sample starts out significantly more polymerized than the less initially condensed sample, there is almost no difference

(36) Christensen, A. N.; Jensen, T. R.; Norby, P.; Hanson, J. C. *Chem. Mater.* **1998**, *10*, 1688.
(37) Clark, S. M.; Kennedy, K. A. *Thermochim. Acta* **1997**, *307*, 27, Clark, S. M.; Kennedy, K. A. *Materials Science Forum* Transtec Publications: Switzerland, 1996; Vols. 228−231.
(38) Chen, J. H.; Weidner, D. J.; Parise, J. B.; Vaughan, M. T.; Raterron, P. *Phys. Rev. Lett.* **2001**, *86*, 4072.
(39) Elmer, J. W.; Wong, J.; Ressler, T. *Scr. Mater.* **2000**, *43*, 751.
(40) Irifune, T.; Nishiyama, N.; Kuroda, K.; Inoue, T.; Isshiki, M.; Utsumi, W.; Funakoshi, K.; Urakawa, S.; Uchida, T.; Katsura, T.; Ohtaka, O. *Science* **1998**, *279*, 1698.
(41) For an example of an unrelated nanoscale system with similar coupling between atomic and nanoscale structure, see: Williams, J. R.; Johnson, M.; Johnson, D. C. *J. Am. Chem. Soc.* **2001**, *123*, 1645. Noh, M.; Johnson, D. C.; Elliott, G. S. *Chem. Mater.* **2000**, *12*, 2894.
(42) Voegtlin, A. C.; Matijasic, A.; Patarin, J.; Sauerland, C.; Grillet, Y.; Huve, L. *Microporous Mater.* **1997**, *10*, 137.
(43) Norby, P. *J. Am. Chem. Soc.* **1997**, *101*, 55215. Norby, P.; Hanson, J. C. *Catal. Today* **1998**, *39*, 301.

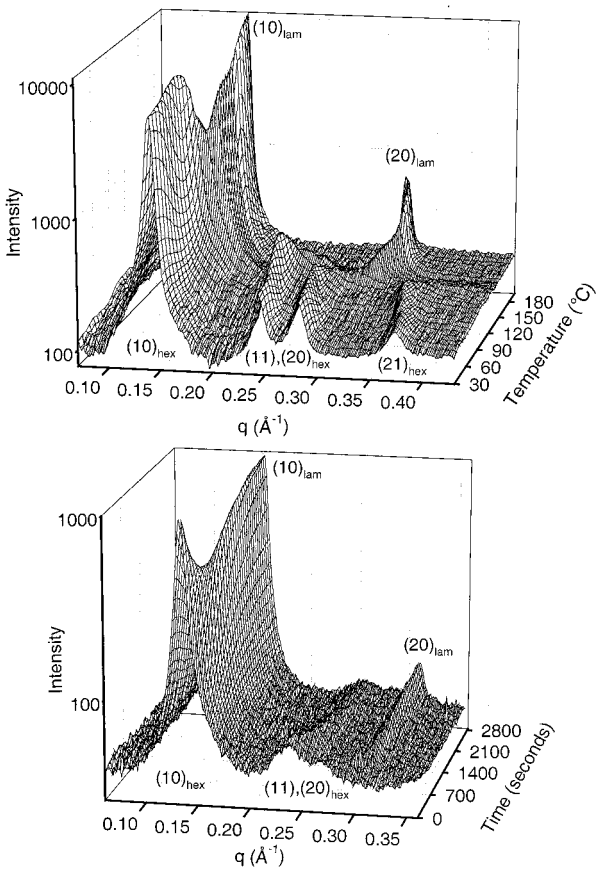

Figure 2. Evolution of diffraction patterns with temperature (top) and time (bottom) for pH 10 ramped and isothermally heated less initially condensed samples. All peaks are indexed on the graphs. In both graphs, a three- or four-peak pattern from a hexagonal phase is initially observed, which transforms into a two-peak pattern indicative of a lamellar phase. The ramped data (top), which are from a sample heated at 4.4 °C/min, show a single sharp transition. The isothermal data (bottom) from a sample held at 113 °C show slower continuous phase evolution with time.

in the value after heating to 100 °C at pH 9. The pH 9 sample has a slightly higher Q^4/Q^3 ratio of 1.41 ± 0.06 compared to 1.34 ± 0.04 for the pH 9c sample (errors are at the 95% confidence level). The larger change in the less initially condensed sample is in part because the more initially condensed sample has fewer adjacent Q^3 silanol species and so condensation may be sterically frustrated.

In Situ Diffraction Data. Figure 2 shows low-angle X-ray diffraction data that are indicative of the data used throughout this work. For these data, less initially condensed samples were hydrothermally heated in a pH 10 buffer. In Figure 2, a four- (top) or three-peak (bottom) pattern is observed that can be indexed to a *p6mm* hexagonal phase. Upon heating this material, it transforms to a two-peak pattern that indexes to a layered lamellar phase. In Figure 2, top, the sample is heated nonisothermally at a linear ramp rate of 4.4 °C/min. The hexagonal peak intensities quickly decrease and the lamellar peaks grow in rapidly around the transition point. By contrast, the isothermal data in Figure 2, bottom, show slow phase evolution for both the hexagonal and lamellar phases with time.

Another way of looking at the data in Figure 2 is to track just the $(10)_{hexagonal}$ and $(10)_{lamellar}$ peak areas. Figure 3 shows these peak areas versus temperature for the data presented in Figure 2, top. As the material progresses through the phase transition, the hexagonal area rapidly falls off as the lamellar

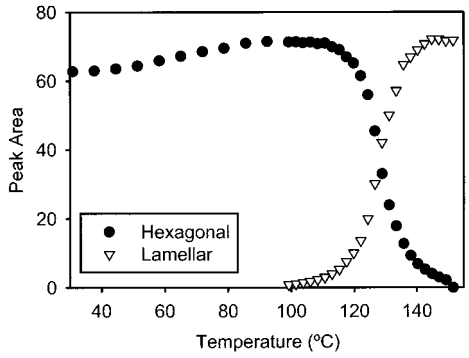

Figure 3. $(10)_{hexagonal}$ and $(10)_{lamellar}$ peak areas for a less initially condensed composite heated in a pH 10 buffer at 4.4 °C/minute. The legend is on the graph. A simple, direct transformation from the hexagonal phase to the lamellar phase is observed.

Table 1: Temperature of Formation of the Lamellar Phase under Nonisothermal (Ramped) Heating

treatment conditions	$T_{transition}$ (°C) at 4.4 °C/min
pH 11	118
pH 10	126
pH 9	167

phase forms. To analyze this kinetic data, it is necessary to define a single phase-transition temperature. We define the halfway point of the hexagonal phase area decrease as the transition temperature. Similar methods are used to define all nonisothermal transition temperatures. Table 1 shows transition temperatures for all pH conditions used in this work on less initially condensed composites heated at 4.4 °C/min.

The data in Table 1 show clear trends with pH. Transition temperatures increase with decreasing pH, demonstrating that a more-condensed sample requires more energy to break the silica framework. Previous studies also indicate that increasingly large amounts of surfactant are lost during hydrothermal treatment at lower pH due to framework condensation;[4] thus, more thermal energy is needed to sufficiently excite the surfactant tails to cause the phase transition at lower pHs. The trends shown in Table 1 are present at all heating rates used in this work. It is interesting to note that if any buffered hydrothermal pH lower than 9 is used, no transformation is observed up to the decomposition temperature of the surfactant (~200 °C). At pHs lower than 9, large amounts of condensation occur and significant surfactant is lost,[4] reinforcing the concept that these two processes inhibit the phase transformation.

Table 1 begins to address the effect of chemistry that occurs during data collection. We are also interested in differences in kinetics caused by chemistry that occurred during formation of the composite. To do this, we looked at the transformation of more initially condensed samples heated in a pH 9 buffer. While these materials begin fairly condensed, they do not show as much silica condensation during heating as a less initially condensed sample treated in a pH 9 buffer (Figure 1)[3,4] because the materials start with fewer reactive silanol groups and have limited framework flexibility. These materials also are synthesized with 25% less surfactant (which provides the driving force for transformation) than a less initially condensed sample.[3] Because of the highly condensed framework, the low pH, and the lower surfactant density, the hexagonal-to-lamellar transition temperature for pH 9c samples heated at 4.4 °C/min is 186 °C. This temperature is higher than for any less initially condensed

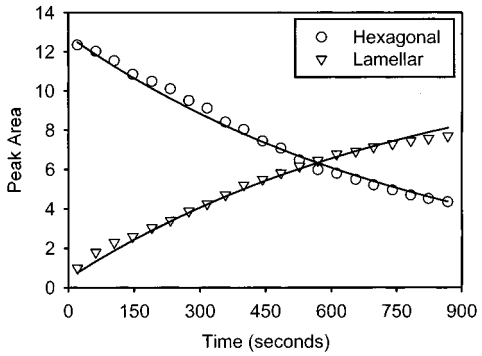

Figure 4. $(10)_{hexagonal}$ and $(10)_{lamellar}$ peak areas for a less initially condensed composite heated at 113 °C in a pH 10 buffer. The legend is on the graph. Black lines show a global fit to peak areas for both phases. A simple, direct progression of the hexagonal phase to the lamellar phase is observed.

samples, once again suggesting that silica condensation and low surfactant concentrations in the composites inhibit the phase transformation.

The same trend of higher transition temperatures for materials heated at lower pHs is also seen in the isothermal experiments. Higher holding temperatures are required to observe significant hexagonal-to-lamellar phase transformation for pH 9 than for pH 10 composites, and both are higher than the temperatures needed for pH 11 materials. This is because the highly polymerized inorganic framework and lower surfactant concentrations resulting from lower-pH treatment are more difficult to transform. The higher holding temperatures compensate for this resistance by increasing the surfactant tail motion. This, in turn, results in a larger surfactant shape change, which can better drive the phase change. An example of the progress of an isothermal phase change is shown in Figure 4. These data are generated from the transition surface shown in Figure 2 (bottom) and were obtained from a less initially condensed composite heated in a pH 10 buffer at 113 °C. The exponential rise of the lamellar phase and exponential loss of hexagonal phase peak area allow for fits to the whole data series, rather than obtaining just a characteristic point, as in the nonisothermal data.

Transformation Mechanisms. The differing amounts of polymerization that occur at different pHs result in multiple chemically accessible transformation mechanisms as the materials transform from a *p6mm* hexagonal phase into a lamellar phase. Figure 5 shows the paths that have been identified in this work. A pH 10 or a pH 9c sample undergoes a simple and direct hexagonal-to-lamellar phase transition like those described above. When more condensation occurs, such as in a pH 9 sample, a hexagonal phase with very condensed walls appears to forms before the material becomes lamellar. Formation of this "annealed" hexagonal phase is supported by the large increase in silica condensation shown in Figure 1 at pH 9. When the least polymerization occurs at pH 11, however, a different phase progression is observed. A pH 11 sample forms a *cmm* centered rectangular phase before becoming lamellar.[15] The *cmm* phase offers a compromise in curvature between hexagonal and lamellar packing. This phase likely occurs because most of the surfactant is retained at high pH and because the less-polymerized framework is easier to deform into the *cmm* structure. As a result, a phase that offers optimal packing of the surfactant such as *cmm* is both energetically necessary and kinetically accessible.

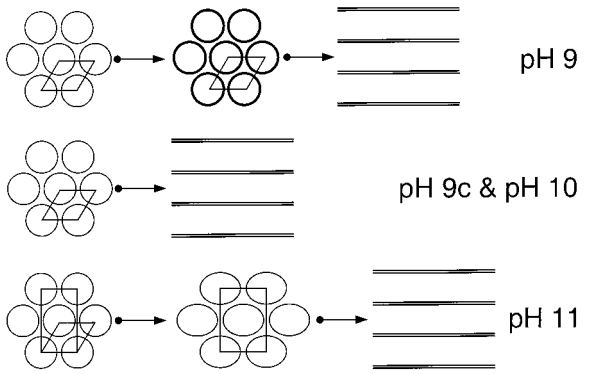

Figure 5. Dependence of the transformation mechanism for a composite material on the treatment pH. Only pH 11 treatment allows the formation of a centered rectangular intermediate phase. Treatment in a pH 9 buffer results in an annealed hexagonal intermediate phase, while pH 9c and pH 10 treatments show simple, direct hexagonal-to-lamellar transformations.

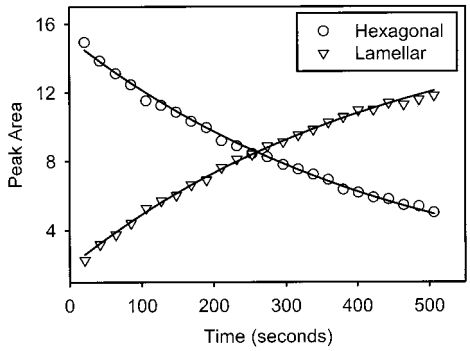

Figure 6. $(10)_{hexagonal}$ and $(10)_{lamellar}$ peak areas for a more initially condensed composite in a pH 9 buffer held at 163 °C (pH 9c). The legend is on the graph. Only the direct hexagonal-to-lamellar transformation is observed. The black lines show a global fit to peak areas for both phases.

Direct transformations occurring during pH 10 and pH 9c treatments (shown in Figures 4 and 6, respectively) are the simplest to analyze by both isothermal and nonisothermal methods. Their single-exponential behavior observed in the isothermal data is indicative of a single transformation process.[15] Neither data from pH 11 nor those from pH 9 samples appear to be single-exponential because of the occurrence of intermediates. Evidence for the formation of an annealed hexagonal phase intermediate during pH 9 treatment is shown in Figure 7. This less initially condensed sample was held at 154 °C in a pH 9 buffer. These data look very different from Figures 4 or 6, because the hexagonal-phase area does not exponentially decrease and because the rise of the lamellar phase now appears to be biexponential. The hexagonal-phase area probably does not decrease as expected because the extraordinarily large amount of condensation causes significant surfactant loss. Surfactant loss has been shown to increase the X-ray contrast of the material, which can result in over a 100% increase in the $(10)_{hexagonal}$ peak area.[4] This effect masks the decrease of the hexagonal phase and makes fitting these data impossible.

We note that it is possible that some condensation-driven surfactant loss could also be affecting the intensity of the lamellar peaks used to generate Figure 7. Most surfactant loss, however, has been shown to occur at lower temperatures,[4] and some additional surfactant loss may be required for the hexagonal-to-lamellar transformation.[16] As a result, we feel confident using the measured lamellar peak areas. In addition,

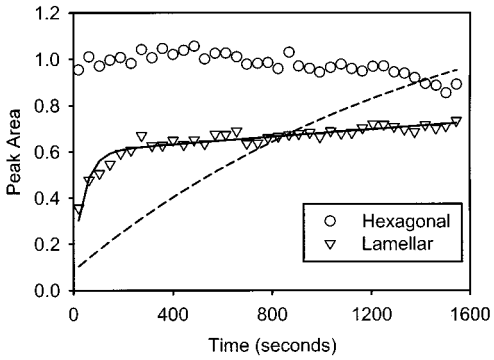

Figure 7. $(10)_{hexagonal}$ and $(10)_{lamellar}$ peak areas for a less initially condensed composite in a pH 9 buffer held at 154 °C. The legend is on the graph. Unlike Figure 5, these data are biexponential, indicating that direct hexagonal-to-lamellar and hexagonal-to-annealed hexagonal-to-lamellar transformations occur simultaneously. A large amount of annealed hexagonal phase was formed during this experiment because the low holding temperature slows the direct hexagonal-to-lamellar phase transformation and gives untransformed hexagonal material time to anneal into a more-condensed, transformation-resistant material. The black solid line shows a biexponential fit to the lamellar peak area data assuming two possible transformation pathways, while the dotted line shows a single exponential fit to the lamellar peak area data, which is clearly not appropriate. The hexagonal-phase data cannot be fit because the hexagonal peak area increases due to increased X-ray contrast caused by surfactant loss during the heating process.

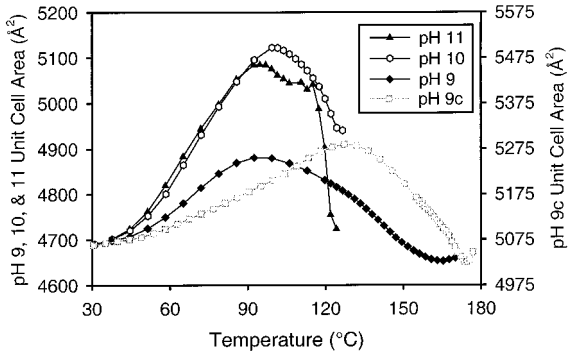

Figure 8. Rectangular unit cell area for less and more initially condensed composites heated at 4.4 °C/min. The legend is on the graph and specifies the pH treatment for each sample. Unit cell areas for the less initially condensed samples are on the left *y*-axis, while the pH 9c unit cell area is shown on the right *y*-axis. The materials heated in pH 10 and pH 11 buffers show the largest change in volume, while a smaller change is observed from the samples heated under pH 9 and pH 9c conditions. A smaller volume increase is seen at lower pH because increased condensation results in reduced surfactant concentration within the composite. Higher temperatures are required to reach maximal volume for the more initially condensed material. The sharp drop in the pH 11 treated sample resulted from transformation to the rectangular phase.

if surfactant is lost and any of the volume is replaced by water, the overall effect on the electron density contrast would be small, so it should not affect the data.[44] Surfactant loss has also been shown to be negligible at high pH,[4] so little effect of any kind should be observed in the higher pH data. In agreement with this, for pHs higher than 9, good agreement is observed between the hexagonal decay and the lamellar rise. It thus appears that surfactant loss only prevents kinetic analysis of the hexagonal phase data for isothermally heated pH 9 samples.

The biexponential appearance of the lamellar-phase area at pH 9 is clear evidence of a complex phase progression involving intermediates. Kinetic data appear to be biexponential only when multiple transformation pathways exist. Because the pH 9c samples have fewer reactive silanol groups and show less polymerization (and almost no surfactant loss[4]) during hydrothermal heating, no annealed hexagonal phase is formed during pH 9c isothermal heating and single-exponential kinetics are observed. This further reinforces the need for significant condensation to form the intermediate annealed hexagonal phase.

The pH 11 data, which are displayed in ref 15, appear to be significantly different from any other pH treatment data. The hexagonal, rectangular, and lamellar phases can all be individually observed, so three populations are shown. At low isothermal temperatures, the hexagonal-to-rectangular transformation finishes before the rectangular-to-lamellar transformation begins and the data are well-described by two single-exponential decays. However, at high isothermal temperatures, the hexagonal-to-rectangular, the rectangular-to-lamellar, and the direct hexagonal-to-lamellar transformations all overlap. In this case, the data are biexponential and appear to be similar to the pH 9 data.

For the nonisothermal pH 11 data, two distinct transitions can be observed indicative of the hexagonal-to-rectangular and rectangular-to-lamellar transitions. By contrast, the complexity of the pH 9 transitions is lost in the nonisothermal data as the regular and annealed hexagonal phases are distinguished only by transition time scale and not by clear difference in diffraction signal. As a result, nonisothermal data for pH 10, pH 9, and pH 9c treatments all look much like the data presented in Figure 3.

pH Control of Surfactant Density. The changes in framework polymerization seen in Figure 1 and the changes in mechanism shown in Figure 5 are indicative of changes in surfactant density in the material. When a surface $Si-O^-$ species that is electrostatically bound to a surfactant condenses with another Q^3 species to form two Q^4 silicas, an OH^- ion is liberated. If this hydroxide ion diffuses away, the surfactant that was bound to the Q^3 site is also released and can escape into solution. Thermal disordering of the surfactant provides a driving force for pore size enlargement and phase rearrangements in these materials.[4,21] When surfactant is heated, its tail becomes thermally excited and increases its volume. This thermal motion both drives the phase transformation and alters the size of the organic domain.[15] Thus changing the amount of surfactant in the composites should change the size of the organic domains and alter the phase-transition temperature.[4] Figure 8 shows unit cell areas as a function of temperature for more and less initially condensed samples heated at 4.4 °C/min. Unit cell area, not unit cell volume, is used because the diffraction data only give information on order in two dimensions in these intrinsically two-dimensional materials. The rectangular unit cell is used because the sample heated in a pH 11 buffer forms an intermediate rectangular phase and a rectangular unit cell can be used to describe both the *p6mm* hexagonal structure and the *cmm* phase, as shown in Figure 5.

All samples in Figure 8 increase in unit cell area and then show a large drop in area. The changes can be related to changes in surfactant density in the material. The pH 10 and 11 treated samples have a large increase in unit cell area, while less change is observed for the pH 9 and 9c treated samples. This is because more condensation occurs at pH 9, which results in more

(44) McMaster, W. H.; Kerr Del Grande, N.; Mallett, J. H.; Hubbell, J. H. *Compilation of X-ray Cross Sections: section II revision I (UCRL-50174SecI)*; National Technical Information Service: Livermore, CA, 1969.

surfactant loss and thus in a smaller expansive force than that present during pH 10 or 11 treatments, where most of the surfactant is retained.[4] The drop in unit cell area seen in all samples is related to the onset of the phase transformation to a lamellar phase. The extra large drop at pH 11 is from the intermediate rectangular phase, which more efficiently accommodates the surfactant packing constraints than the hexagonal phase.[15] The end of the data for each pH treatment in Figure 8 indicates the 50% transition point. The pH 9 treated sample transforms at a considerably higher temperature than the higher pH samples because less surfactant is present to promote the phase transformation and because the more condensed framework at pH 9 (Figure 1) is harder to rearrange.

Additional insight about the importance of initial condensation can be gained by comparing the more and less initially condensed data in Figure 8. The pH 9c peak in unit cell area occurs ~30 °C higher than the peaks of the pH 9−11 samples (which all appear at around the same temperature). This difference reflects the increased condensation and reduced surfactant concentration in more initially condensed materials at low temperature (before significant hydrothermal treatment). By contrast, the pH 9 and pH 9c samples show approximately the same total unit cell area increase, which agrees well with the similarities in the final degree of framework condensation (Figure 1). Previous studies show that pH 9 samples lose a significant amount of surfactant, while pH 9c samples lose almost none.[4] Because the pH 9c sample starts with less surfactant, however, both samples probably end with similar silica/surfactant ratios. It appears that that the final physical state of the material, which is very close for pH 9 and 9c samples, determines the amount of lattice expansion while the starting configuration has a greater influence on the time course of the changes. The direct change in atomic-scale polymerization and the indirect change of surfactant loss caused by silica chemistry will be themes used to explain data throughout the rest of this work.

Discussion

The chemical changes shown in Figure 1 and the altered transition temperatures shown in Figure 8 and Table 1 suggest that chemistry during the heating ramp can fundamentally alter the atomic scale structure of these silica/surfactant composites. These changes should, in turn, modify the metastability of the resulting hexagonal phase. To quantify these changes in terms of kinetic stability, we use the peak area data presented in Figures 5−7 to calculate activation energies for the observed structural rearrangements. Comparison of our activation energies will provide insight into the role of chemistry in modifying the ease of rearrangement of these materials. The ramped (nonisothermal) data will be analyzed using the Ozawa equation,[33] while the isothermal data will be analyzed with the Avrami rate law and Arrhenius kinetics.[45] Because these materials can show structural changes on multiple length scales (atomic and nanometer), it is not clear whether both of these kinetic formalisms are applicable to a complex system such as this one. The results of each analysis will be compared to identify how chemistry that occurs during heating differently affects the results obtained from each method.

(45) Avrami, M. *J. Chem. Phys.* **1939**, *7*, 1102; **1940**, *8*, 212; **1941**, *9*, 177.

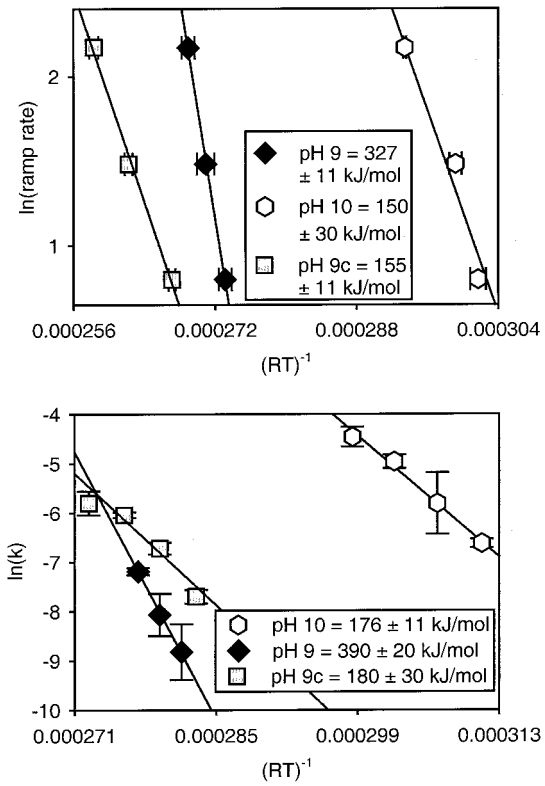

Figure 9. Data from less initially condensed samples heated in pH 10 (white hexagons) and pH 9 (black diamonds) buffers and data from more initially condensed samples heated in a pH 9 buffer (grey squares): (top) averaged nonisothermal data fit to the Ozawa equation for the hexagonal-to-lamellar transformation; (bottom) averaged isothermal data fit to the Arrhenius equation for the hexagonal-to-lamellar transformation. Apparent activation energies for each pH and sample are shown on the graphs.

Nonisothermal Kinetic Analysis. It has been shown that it is possible to relate the midpoints of phase transitions measured while heating at different linear ramp rates to the activation energy for transformation.[33] Ozawa expressed the relationship as follows:

$$\ln(b) = -\frac{E_a}{RT} + \text{int}$$

where b is the ramp rate, E_a is the activation energy, R is the gas constant, and T is the absolute transition temperature. The term "int" is the intercept of the plot, which contains information about the Arrhenius preexponential factor (A), but which also contains constants obtained by integrating a rate law over temperature to produce an equation in "b" rather than "k". As a result, the A factor cannot be simply obtained from the intercept data. We use the Ozawa equation because it describes many phase-change processes well and because it has been shown to produce reasonable agreement with isothermal[33,34] and other nonisothermal methods.[46] Each experimental nonisothermal run gives a (b, T) point; multiple runs with different ramp rates on the same sample are used calculate the activation energy for transformation.

Figure 9 (top) shows Ozawa equation fits to data like those presented in Table 1 (but including many heating ramp rates). All data points are the averages of 2−3 experimental runs, and apparent activation energy values are shown on the plot. We

(46) Tiernan, M. J.; Barnes, P. A.; Parkes, G. M. B. *J. Phys. Chem. B* **1999**, *103*, 6944.

use the term "apparent" because of the complex nature of the transformation and the fact that it is not clear what step of the transformation (local silica hydrolysis, coordinated silica hydrolysis, the actually nanoscale rearrangement, etc.) is dominating the kinetic barrier. The annealed hexagonal-to-lamellar phase transition at pH 9 has the highest apparent activation energy of 327 ± 11 kJ/mol, the pH 10 hexagonal-to-lamellar activation energy of 150 ± 30 kJ/mol is lower, and the pH 11 hexagonal-to-rectangular and rectangular-to-lamellar activation energies of 104 ± 7 and 147 ± 7 kJ/mol, respectively, are the lowest. The Ozawa plots for pH 11 data are shown in Figure 6 (top) in ref 15. These results show that condensation during heating at lower pH inhibits the phase transformation, in agreement with the fundamental predictions of silica chemistry. Surprisingly, the more initially condensed sample treated in a pH 9 buffer has an apparent activation energy of only 155 ± 11 kJ/mol. The more initially polymerized framework and lower initial surfactant concentration should make it intrinsically harder for this material to transform.[3] However, the inability of the pH 9c sample to undergo as much condensation during hydrothermal heating as the pH 9 sample (Figure 1) appears to have a greater effect on the final activation energy. This result underscores the huge effect that condensation during heating can have on phase stability.

While the term "apparent activation energy" underscores the fact that the exact molecular basis for the measured values is not know, a reasonable knowledge of silica chemistry allows us to speculate about the data. The hexagonal and lamellar phases have a group/subgroup relationship (i.e., they are suitable for a second-order phase transition).[16] Because of the structural compatibility of the phases, nucleation of the lamellar phase is not likely to be the rate-limiting step in the transition. Chemically, however, hydrolysis appears to be necessary for all of the phase transitions explored here. Activation energies for dissolution of silica range from 61 to 88 kJ/mol for the pHs used in this work.[47,48] These values are smaller than our measured activation energies, suggesting that multiple Si−O−Si bonds need to break in a coordinated fashion to enable rearrangement of the organic domains. Figure 1 demonstrates that a large amount of condensation occurs during heating at lower pH, so more hydrolysis is needed to reverse this effect at lower pH. In addition, because silica hydrolysis is endothermic with an enthalpy of reaction of 15.5 kJ/mol, no energy is released from reaction to help activate further hydrolysis and thus larger activation energies are expected.[49] While the repacking of the surfactant into the lamellar structure likely requires energy as well, this repacking involves modification of weaker electrostatic interactions rather than breaking covalent bonds, thus surfactant repacking is probably less important than inorganic bond breaking in determining silica/surfactant composite-phase transition activation energies. For example, our estimates of the activation energy for a cubic-to-inverse hexagonal phase transition in a pure liquid crystal phase from in situ kinetic data[50] produce a value of E_a near 25 kJ/mol. Disorder−order transitions, such as the formation of a smectic phase from the melt, also show low activation energies (~6.4 kJ/mol).[51] Therefore, the apparent activation energies determined in this work are likely dominated by the energy required to break sufficient Si−O−Si bonds so that rearrangement of the silica walls can occur.

Scheme 1

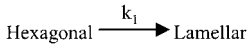

Scheme 2

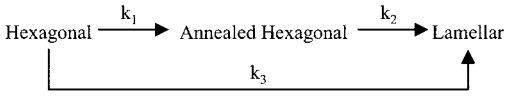

We note that our activation energies are reasonable in terms of other metal oxide solid−solid phase transformations. For example, the γ-Al_2O_3 to α-Al_2O_3 phase transformation has an activation energy of 485 ± 21 kJ/mol, while the olivine-to-spinel transformation in Mg_2GeO_4 has an activation energy of 205 kJ/mol.[52,53] The calculated activation energies in this work also compare very favorably to activation energies in solid−solid phase transformations in other nanostructured materials.[54]

Isothermal Kinetic Analysis. To analyze isothermal kinetic data, a rate law is needed. Atomic scale chemical reactions utilize rate laws that are frequently fairly obvious. For this solid-state rearrangement, we cannot count changes in reactant and product molecules, so we use a rate law that describes a volume-to-volume transformation known as the Avrami rate law. The rate constant is related to the fraction of material transformed as a function of time and a dimensionality parameter.[45]

$$\ln(1 - \alpha) = (kt)^n$$

Here α is the fraction transformed, k is the rate constant for the transformation, t is the time, and n indicates the dimensionality of the phase transition. This equation has been found to describe a wide range of solid−solid phase transformations. The hexagonal-to-lamellar transformation in silica/surfactant composites has been shown to transform with $n = 1$ (i.e., the transformed lamellar volume grows in one direction, rather than spreading as a disk or a sphere).[3,15] We will use this value for hexagonal-to-lamellar, hexagonal-to-annealed hexagonal-to-lamellar, and the related rectangular-to-lamellar transitions studies here.[3,15]

The simple hexagonal-to-lamellar phase rearrangement occurring in pH 10 and pH 9c samples as pictured in Figure 5 (middle) can be described by Scheme 1. An example of fitting to this model is seen in the black lines in Figure 4 and Figure 6. The hexagonal-to-lamellar rate constant is k_1. To achieve a better fit to the data, the hexagonal and lamellar phase areas are fit together. The high fit quality suggests that we are using the correct transition mechanism.

More complex phase behavior is seen in Figure 7. A function can be derived to fit the lamellar data on the basis of the two pathways shown in Scheme 2. Here, the hexagonal-to-annealed hexagonal transformation has the rate constant k_1, the annealed hexagonal-to-lamellar transformation has the rate constant k_2, and the direct hexagonal-to-lamellar transformation has the rate

(47) Rimstidt, J. D.; Barnes, H. L. *Geochim. Cosmochim. Acta* **1980**, *44*, 1683.
(48) Niibori, Y.; Kunita, M.; Tochiyama, O.; Chida, T. *J. Nucl. Sci. Technol.* **2000**, *37*, 349.
(49) Fournier, R. O.; Rowe, J. J. *Am. Mineral.* **1977**, *62*, 1052.
(50) Caffrey, M. *Biochemistry* **1987**, *26*, 6349.
(51) Pardey, R.; Wu, S. S.; Chen, J.; Harris, F. W.; Cheng, S. Z. D.; Keller, A.; Aducci, J.; Facinelli, J. V.; Lenz, R. W. *Macromolecules* **1994**, *27*, 5794.
(52) Steiner, C. J.-P.; Hasselman, D. P. H.; Spriggs, R. M. *J. Am. Ceramic Soc.* **1971**, *54*, 412.
(53) Lauterjung, J.; Will, G. *Physica B* **1986**, *139−140*, 343.
(54) Chen, C. C.; Herhold, A. B.; Johnson, C. S.; Alivisatos, A. P. *Science* **1997**, *276*, 398.

Table 2: pH 9 Transformation Rate Constant Ratios

T (°C)	k_3/k_1
154	0.49
157	0.57
160	0.85

Scheme 3

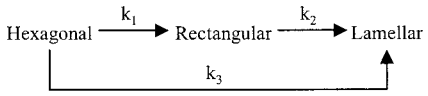

constant k_3. The full derivation of the kinetic functional form (derived for an analogous system) is available elsewhere.[15] The annealed hexagonal-to-lamellar and the direct hexagonal-to-lamellar pathways and their respective rates account for the biexponential nature of the data in Figure 7. The nice agreement between the black line in Figure 7 and the data suggests that our model was chosen correctly. The dotted line in Figure 7 shows a single-exponential fit (which extrapolates to the correct long-time limits) for the lamellar phases data. It is clear that a direct phase transformation, which would give single-exponential behavior, does not agree with the data.

We also find meaningful trends with temperature for the rate constants along the direct hexagonal-to-lamellar and the two-step hexagonal-to-annealed hexagonal-to-lamellar pathways as shown in Table 2. The k_3 path is accelerated at higher temperature relative to the two-step k_1-k_2 pathway because less-annealed hexagonal material can be formed before the original hexagonal phase is consumed.

The k_3 path is thus the higher energy pathway, which is more accessible at higher temperature. Figure 7 shows data taken at the lowest heating temperature used in these experiments in which there is very clear biexponential behavior. Unfortunately, at higher holding temperatures, some of the initial transformation occurs during the isothermal heating jump, so the k_1 and k_3 rate constants are not determined accurately enough to calculate a meaningful activation energy for the direct transformation. Because of the details of the integrated rate law,[15] however, the k_3/k_1 ratio can be determined more accurately than k_1 or k_3 alone.

Less initially condensed samples heated at pH 11 also exhibit a complex transformation mechanism, which is shown in Figure 5 and Scheme 3. This mechanism has been extensively discussed elsewhere and is mathematically the same as that used for pH 9 materials.[15] As with the pH 9 treated less initially condensed samples, the k_1/k_3 ratio depends on temperature and, again, the direct higher energy hexagonal-to-lamellar pathway is accelerated relative to the two-step process at higher temperature. Thus, the amount of material transforming by the direct route should decrease until at very low temperature, the direct path is no longer kinetically accessible, a fact which is experimentally observed.

A summary of all transformations and their relative rate constants is shown in Table 3. Very different holding temperatures were used for each sample, so we use the nonisothermal transition point to effectively normalize the transition temperatures. All rate constants shown in Table 3 were measured at a temperature that is approximately 9 °C below the 2.2 °C/min nonisothermal transformation temperature. Presented in this way, some trends emerge from the data. For example, the rate constant for the annealed hexagonal-to-lamellar transformation at pH 9 (k_2) is significantly smaller than the related hexagonal-to-lamellar rate constants for pHs 10, 11, and 9c (k_1, k_3, and k_1, respectively), demonstrating the effect of condensation during heating. Comparisons within a sample also show how different amounts of chemistry during heating can affect rate constants. While it is important to remember that the relative values of the rate constants presented for the pH 9 and 11 samples are a strong function of temperature, at the temperatures shown, some interesting trends can be observed. For pH 11 materials in which little condensation during heating occurs, the direct hexagonal-to-lamellar rate constant (k_3) is only 8 times higher than the rectangular-to-lamellar rate constant (k_2). For the pH 9 material, by contrast, the hexagonal-to-lamellar rate constant (k_3) is almost 150 times higher than the annealed hexagonal-to-lamellar rate constant (k_2). The silica condensation that produces the annealed hexagonal phase also dramatically changes the rate constant for transformation to the lamellar phase.

When rates constants are known at a variety of isothermal temperatures, activation energies can be found using the Arrhenius equation.

$$\ln k = -\frac{E_a}{RT} + \ln A$$

where k is the rate constant, E_a is the activation energy, R is the gas constant, T is the absolute temperature, and A is the Arrhenius preexponential factor. The Arrhenius fits are shown in Figure 9 (bottom) and in Figure 6 (bottom) in ref 15. Activation energies are shown on each plot and are summarized in Figure 10. Again, pH 9 samples show the highest apparent annealed hexagonal-to-lamellar activation energies (390 ± 20 kJ/mol), a lower hexagonal-to-lamellar apparent activation energy is observed for pH 10 samples (176 ± 11 kJ/mol), and the lowest rectangular-to-lamellar apparent activation energy is observed for pH 11 composites (140 ± 20 kJ/mol). The hexagonal-to-lamellar activation energy for pH 9c materials (180 ± 30 kJ/mol) is once again very similar to the E_a for pH 10 composites. No hexagonal-to-intermediate or direct hexagonal-to-lamellar activation energies are given for pH 9 or pH 11 samples because the bulk of these transformations occur so quickly that there are insufficient data to fit after the material has equilibrated at the set temperature.

Interestingly, the Arrhenius preexponential is found to correlate with the measured activation energy as shown in Table 4. This clear increase in A with increasing activation energy has been observed in many solid-state reactions and is known

Table 3: Relative Isothermal Reaction Rate Constants

phase change	nonisothermal T_{trans} (°C)	log(k_1)	log(k_2)	log(k_3)
pH 11, hexagonal-to-rectangular-to-lamellar	109	−2.05	−3.24	−2.72
pH 10, hexagonal-to-lamellar	117	−2.67		
pH 9, hexagonal-to-annealed hexagonal-to-lamellar	158	−0.96	−3.39	−1.20
pH 9c, hexagonal-to-lamellar	168	−2.52		

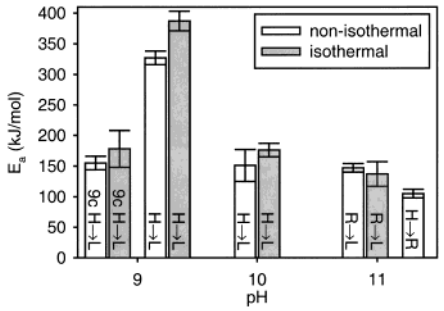

Figure 10. A strong dependence on treatment pH is observed in both the apparent activation energies and the type of transition that occurs. The type of phase change is shown on each bar (H = hexagonal, R = rectangular, and L = lamellar), and the kinetic method utilized is shown in the legend. All activation energies are for less initially condensed composites except for those labeled 9c, which are for more initially condensed samples. Activation energies increase with decreasing pH, demonstrating that condensation inhibits the phase transformation. This idea is reinforced by consideration of pH 9c composites. These materials cannot undergo significant condensation during heating and thus show a lower activation energy for transformation.

Table 4: Preexponential Factors and Activation Energies for Less Initially Condensed Composites

treatment pH	ln A (ln s^{-1})	activation energy (kJ/mol)
9	100 ± 4	390 ± 20
10	48 ± 3	176 ± 11
11	39 ± 6	140 ± 20

as the kinetic compensation effect.[55−60] When activation energies are dramatically altered by changing reaction conditions in a chemical system, the A factor has been observed to track the change in activation energy according to the following empirical relationship:

$$\ln A = b \ln E_a + c$$

where b and c are constants. When our data is fit to this relationship, we find $b = 0.246 \pm 0.001$, $c = 5.03 \pm 0.02$, and an R^2 regression statistic of 0.99996, reinforcing the idea that the kinetic compensation effect describes our data well. The kinetic compensation effect is mainly found in solid-to-solid/gas decompositions and in heterogeneous catalysis. Both are systems in which the relative reactant and product energies, and thus the activation energy for the process, can be dramatically tuned by changing the gas pressure. We have already shown that silica/surfactant composites are a unique system in which solution-phase chemistry can be used to tune the apparent activation energy, so it is not surprising that we also see the kinetic compensation effect. While the theoretical basis for the effect is not entirely clear, it is reasonable that a much smaller fraction of attempted transformations are successful when the transition barrier is high, and thus a higher attempt frequency is needed to observe measurable rates.

Trends in Activation Energies. Figure 10 provides a summary of all activation energies calculated for these composites using both isothermal and nonisothermal methods. It can be seen that for a given synthesis condition as the treatment pH decreases there is an increase in activation energy. Condensation of silica bonds is more rapid at lower pH, so the activation energies are simply correlated with silica chemsitry.[23] The root of this correlation lies in the fact that bonds need to be broken for a structural arrangement to occur and thus more coordinated bond breaking should produce higher activation energies. For example, the hexagonal-to-rectangular transformation for pH 11 samples has the lowest activation energy because this change is just a deformation of the framework and should require less bond breaking. On the other hand, the pH 9 annealed hexagonal-to-lamellar phase transition requires the most bonds to be broken (Figure 1) for a transition to occur, and thus, it has the highest activation energy.

The trend of higher activation energies for more condensed samples does not continue, however, when comparing pH 9 and pH 9c composites. Figure 1 indicates that pH 9 composites show very similar degrees of condensation to pH 9c composites, while the differences in activation energies are extremely large. To understand this trend, we need to think not only about the total degree of condensation but also about how that condensation is correlated with the strain of the silica network and the nanoscale architecture of the composite. It should be noted that in bulk silica, it has been shown that the activation energy for single hydrolysis events appears to be correlated with the strain in the silica network.[61]

As synthesized, the silica framework apparently has high- and low-density regions, but upon hydrothermal heating, diffraction modeling suggests that the framework achieves a more uniform silica density, mostly through increased condensation of the low-density regions.[4,13,14,62,63] Thinning of the silica walls, also correlated with silica condensation, can produce similar changes in the diffraction patterns.[64] We refer to this structural change, in which the silica framework becomes more uniform and denser, as "annealing". Annealing can be observed by examining changes in the relative intensities of the nanoscale Bragg diffraction peaks, in particular in the $(11)_{hexagonal}/(20)_{hexagonal}$ integrated peak area ratio. As shown in Figure 2, these peaks have almost equal peak areas before hydrothermal treatment, but after heating and before the phase transition, the $(11)_{hexagonal}$ peak has significantly grown in intensity relative to the $(20)_{hexagonal}$ peak.[2,3,4,13] A greater increase in the $(11)_{hexagonal}/(20)_{hexagonal}$ ratio correlates with more restructuring of the silica walls. Changes in annealing can be used to help explain the difference in activation energies between pH 9 and pH 9c samples.

A pH 9c sample has been shown to anneal less than a pH 9 sample.[4] This difference was attributed to the decreased flexibility in the framework of the more initially condensed sample and thus to an inability to restructure the framework without excessive strain building up.[4] While the pH 9c sample begins more polymerized, the two samples end up with about the same degree of condensation. For the pH 9 material, however, that condensation occurs while the sample is in the hexagonal phase,

(55) Koga, N. *Thermochim. Acta* **1994**, *244*, 1.
(56) Galwey, A. K.; Brown, M. E. *Thermochim. Acta* **1997**, *300*, 107.
(57) Gallagher, P. K.; Johnson, D. W. *Thermochim. Acta* **1976**, *14*, 255.
(58) Zsabó, J.; Arz, H. E. *J. Therm. Anal.* **1974**, *6*, 651.
(59) Galwey, A. K. *Adv. Catal.* **1977**, *26*, 247.
(60) Bamford, C. H., Tipper, C. P. H., Eds. *Reactions in the Solid State*; Comprehensive Chemical Kinetics, Vol. 22; Elsevier: New York, 1980.
(61) Van Ginhoven R. M. PhD. Thesis, University of Washington, 2002.
(62) Lindén, M.; Blanchard, J.; Schacht, S.; Schunk, S. A.; Schüth, F. *Chem. Mater.* **1999**, *11*, 3002.
(63) Schacht, S.; Janicke, M.; Schüth, F. *Microporous Mesoporous Mater.* **1998**, *22*, 485.
(64) Feuston B. P.; Higgins J. B. *J. Phys. Chem.* **1994**, *98*, 4459.

Table 5: Effect of Heating Profile on Annealing

treatment conditions	isothermal		nonisothermal	
	T (°C)	$(11)_{hex}/(20)_{hex}$	heating rate (°C/min)	$(11)_{hex}/(20)_{hex}$
pH 9	154	3.89 ± 0.09	2.2	3.00 ± 0.10
	157	3.94 ± 0.11	4.4	2.88 ± 0.06
	160	4.22 ± 0.11	8.8	2.80 ± 0.14
pH 10	113	3.14 ± 0.09	2.2	2.23 ± 0.10
	119	3.18 ± 0.08	4.4	2.05 ± 0.14
	124	3.53 ± 0.13	8.8	2.28 ± 0.26

so the condensation specifically results in a more homogeneous less strained, and thus more hydrolytically stable material. For the pH 9c composite, in which most of the condensation occurs during solution-phase synthesis, the silica walls are probably still inhomogeneous and strained despite the fact that they are well-condensed. As a result, it is much easier to break bonds in a pH 9c material and thus, rearrange into the lamellar phase than a pH 9 composite.[61]

Comparison of Isothermal and Nonisothermal Data. Our confidence in all of the values calculated in this paper is bolstered by the remarkable agreement between the nonisothermal and isothermal kinetic methods. With the exception of pH 9 composites, all activation energies agree within experimental error, and the absolute difference in methods for pH 9 samples is only 16%. The difference for pH 9 samples appears to be statistically significant, however, so it is worthwhile to consider the basis for the discrepancy.

For these silica/surfactant composites, structural changes can occur on both atomic and nanometer length scales. Symmetry does not tie these length scales together, so any amount of silica condensation or hydrolysis can occur prior to a nanoscale rearrangement. It is thus likely that the difference between isothermal and nonisothermal methods stems from differences in the amount of chemistry that occurs during the heating profiles. Fundamentally, neither kinetic method is capable of accounting for chemistry that occurs prior to the phase change; the rate equations assume a fixed initial state that transforms to a fixed final state. Understanding this chemistry is thus very important for interpreting our results. In a nonisothermal process, significant reaction time is available as the material is heated to the transition temperature. Much less time is available during an isothermal temperature jump and hold, although the sample does spend whatever time it has at a significantly higher temperature. We will use changes in the relative intensities of the diffraction peaks (annealing) as a measure of the differences in chemistry that occur during the two heating profiles. By comparing the methods and their results, we hope to gain insight into which model is better suited to complex systems that can rearrange on multiple length scales.

To examine restructuring of the inorganic phase of the composite, we can consider how the amount of annealing varies with ramp rate or temperature before the transformation has significantly progressed on less initially condensed samples (Table 5). The data from pH 9 samples show a trend in annealing under both isothermal and nonisothermal conditions. Increased annealing with slower ramps is reasonable because a longer ramp will provide more time for condensation to occur. A greater extent of annealing also results from higher isothermal holding temperatures. Annealing is a kinetically limited process, and the extra available energy at a higher holding temperature appears to allow more annealing to proceed before the material transforms. While no trend is present in the pH 10 nonisothermal data, the same trend exists in the pH 10 isothermal data as that in the pH 9 isothermal data. There may be no obvious trend in the pH 10 nonisothermal data because less total annealing occurs at pH 10 compared to pH 9.

When trends exist in annealing with holding temperature or ramp rate, the measured rate constants and transition points can be artificially shifted, resulting in errors in the calculated activation energies. According to Table 5, for the pH 9 nonisothermal measurements, slower-ramp-rate samples are more annealed. This makes slow-ramp-rate samples harder to transform, which in turn will raise their transition temperatures, thus making the calculated activation energy appear lower than its true value. Because no trend exists in annealing in the nonisothermal pH 10 data, where less chemistry occurs, we assume that the pH 10 and 11 activation energies are not significantly biased. However, the trend in annealing for isothermal data collected at both pH 9 and 10 will produce artificially low activation energies because the highest hold temperatures should have chemically slowed reaction rates. At pH 9, the extent of differential annealing during heating is approximately the same for both the isothermal and nonisothermal data. As a result, both activation energies should be artificially lowered by a similar amount, so this effect cannot explain the difference between isothermal and nonisothermal activation energies. The results do suggest, however, that the true difference in activation energies between the lowest and highest pH treatments might be even greater than that shown in Figure 10.

To understand the differences between activation energies measured by isothermal and nonisothermal methods, we need to look at not just the changes but also the absolute values of the $(11)_{hexagonal}/(20)_{hexagonal}$ area ratios. The amount of annealing for isothermal samples is significantly higher than that for ramped samples for both pHs (Table 5). This results in higher isothermal activation energies in all experiments (although pH 11 is not statistically different). Simply put, isothermally heated composites are more annealed prior to rearrangement and thus harder to transform. Treatment at pH 9 shows the largest difference in activation energies between methods because the most condensation occurs at this pH. The fact that all activation energies agree reasonably well across a wide range of treatment conditions suggests that artificial chemical modification of the calculated values discussed above is not considerable. Instead, the small differences in activation energies represent real chemical differences in the samples.

The results suggest that both isothermal and nonisothermal methods can be successfully applied, even to complex systems such as the inorganic/organic composites studies here. The results obtained from each method may not be identical, however, because the amount of chemistry that occurs during heating is a detailed function of the thermal profile. This chemistry during data collection can change the measured activation energies in a real and meaningful manner. In fact, comparison of isothermal and nonisothermal activation energies provides a good measure of the range of activation energies that can be obtained simply by modifying the thermal profiles.

Conclusions

The rate constants and activation energies calculated in this work emphasize the importance of condensation during heating in controlling phase stability in silica/surfactant composites. Lower treatment pH, where the most condensation occurs, results in the highest activation energies for structural rearrangement with a smooth trend of decreasing activation energy with increasing pH. Condensation that occurs during synthesis, however, has a different effect than condensation during heating on nanoscale metastability. Condensation that occurs during synthesis is less correlated with nanometer scale structure and thus does not effectively stabilize the composites against hydrothermal rearrangements. Materials that are well-condensed during synthesis are unable to undergo significant condensation during heating because of higher strain the low density of reactive bonds. Thus, activation energies for rearrangement remain low in these more initially condensed composites, despite hydrothermal treatment under conditions that should encourage condensation during heating. By contrast, condensation that occurs during hydrothermal treatment of less initially condensed materials results in a more homogeneous less strained silica wall structure and significantly increased hydrothermal phase stability.

The presence or lack of condensation also allows a variety of new energetic pathways to be opened. When very little condensation occurs, almost of all the surfactant is retained. The more flexible framework deforms into a centered rectangular phase to better accommodate the surfactant volume before the rectangular-to-lamellar transformation. By contrast, pH 9 treatment of a less initially condensed composite results in a very condensed, annealed hexagonal phase that is extremely resistant to transformation. This demonstrates the usefulness of reaction chemistry in controlling the final phase of a nanostructured material. In addition, by changing temperature/available energy, it is possible to direct the material to a specific pathway by altering the relative reaction rates for all possible paths. This conclusion has exciting implications for the synthesis of new materials through phase-transition processes.[16−20]

There is, however, a fundamental problem with kinetic studies of nanoscale systems in which nanoscale changes can occur independently of atomic scale changes, and both nonisothermal and isothermal kinetic methods are hindered by the same problems. Despite the fact that the fundamental assumption of an identical starting and ending state is not obeyed in these materials, the results are still quite interpretable and provide meaningful insight into chemistry during a heating process. Activation energies show excellent agreement between isothermal and nonisothermal methods at high pH, and the small differences between isothermal and nonisothermal results at lower pHs can be explained by different amounts of annealing with different heating profiles. The differences in activation energies are not erroneous; rather they represent different physical states of the material just prior to transformation. Therefore, when investigating complex nanoscale systems, it is important to quantify how the material changes prior to the transformation to understand the affect of various heating profiles. It appears for silica/surfactant composites that both kinetic methods are reasonable and that both should be used to better understand the affect of thermal profiles on composite structural rearrangement.

Acknowledgment. A. E. Riley is thanked for help with data collection. This manuscript includes data collected at the Stanford Synchrotron Radiation Laboratory (SSRL), which is operated by the Department of Energy, Office of Basic Energy Sciences. This work made use of equipment supported by the National Science Foundation under Grant DMR-9975975. This work was supported by the National Science Foundation under Grant DMR-9807190. S.H.T. is an Alfred P. Sloan Foundation Research Fellow.

JA0169668